

FAILURE CRITERIA FOR FRP LAMINATES IN PLANE STRESS

Carlos G. Dávila

Aerospace Engineer, Analytical and Computational Methods Branch, Senior Member, AIAA.
NASA Langley Research Center, Hampton, VA 23681

Navin Jaunky

Senior Scientist, National Institute of Aerospace, Member, AIAA.
Hampton, VA 23666

Sanjib Goswami

National Research Council Research Associate.
NASA Langley Research Center, Hampton, VA 23681

Abstract

A new set of failure criteria for fiber reinforced polymer laminates that are being developed at NASA Langley Research Center is described. Derived from Hashin's criteria for unidirectional laminates and Puck's action plane concept, the physically based LaRC02 criteria predict matrix and fiber failure accurately without requiring curve-fitting parameters. For matrix failure under transverse compression, the fracture plane is calculated by maximizing the Mohr-Coulomb effective stresses. A criterion for fiber kinking is obtained by calculating the fiber misalignment under load, and applying the matrix failure criterion in the coordinate frame of the misalignment. The criteria are applied to a few examples to predict failure load envelopes and to predict the failure mode for each region of the envelope. The analysis predictions are compared to the predictions of other available failure criteria and with experimental results. Predictions with LaRC02 correlate well with the experimental results.

Introduction

The aim of damage mechanics, the mathematical science dealing with quantitative descriptions of the physical events that alter a material when it is subjected to loads, is to develop a framework that describes the material response caused by the evolving damage state. The greatest difficulty in the development of an accurate and computationally efficient numerical procedure to predict damage growth has to do with how to analyze the material micro-structural

changes and how to relate those changes to the material response. Several theories have been proposed for predicting failure of composites. While significant progress has been made in this area, there is currently no single theory that accurately predicts failure at all levels of analysis, for all loading conditions, and for all types of fiber reinforced polymer (FRP) laminates. While some failure theories have a physical basis, most theories represent attempts to provide mathematical expressions that give a best fit of the available experimental data in a form that is practical from a designer's point of view.

To the structural engineer, failure criteria must be applicable at the level of the lamina, the laminate, and the structural component. Failure at these levels is often the consequence of an accumulation of micro-level failure events. Therefore, it is also necessary to have an understanding of micro-level failure mechanisms in order to develop the proper failure theories.

The World Wide Failure Exercise (WWFE) conceived and conducted by Hinton and Soden¹⁻⁷ provides a good picture of the status of currently available theoretical methods for predicting material failure in fiber reinforced polymer composites. The recently published comparison of the predictions by the WWFE participants with experimental results indicates that even when analyzing simple laminates that have been studied extensively over the past 40 years, the predictions of most theories differ significantly from the experimental observations.³

The uncertainty in the prediction of initiation and progression of damage in composites has led to the

This material is a work of the U.S. Government and is not subject to copyright protection in the United States.

undertaking of an effort at Langley Research Center to revisit existing failure theories and to develop new ones where necessary. The well-established failure criteria were revisited and their prediction capabilities were compared and their qualities were examined.

This paper describes a newly developed set of non-empirical criteria for predicting failure of unidirectional FRP laminates that is derived from Puck's action plane concept. All the calculations shown here are at the lamina level with plane stress assumptions. First, a new criterion for matrix shear and compression is presented. Then, a fiber kinking failure criterion for fiber compression is developed by applying the matrix failure criterion to the configuration of the kink. Finally, some examples of failure envelopes are presented. The predicted results are compared to the results of other available failure criteria as well as with experimental results.

Strength-Based Failure Criteria

Strength-based criteria are commonly used with the finite element method to predict failure events in composite structures. A large number of continuum-based criteria have been derived to relate internal stresses and experimental measures of material strength to the onset of failure. In the following sections, the Hashin criteria are briefly reviewed, and improvements proposed by Sun and Puck over Hashin's theories are examined.

Hashin Criteria 2D (1980)

Hashin^{8,9} can be credited with establishing the need for failure criteria based on failure mechanisms. In the work in 1973, he used his experimental observations of tensile specimens to propose two different failure criteria, one related to fiber failure and the other related to matrix failure. The criteria assume a quadratic interaction between the tractions associated with the plane of failure. In 1980, he introduced fiber and matrix failure criteria that distinguish between tension and compression failure. Given the difficulty in obtaining the plane of failure in the 3D case, Hashin developed the more recent criteria using a quadratic interaction between stress invariants. Such derivation was based on logical reasoning rather than

micromechanics. Although they were developed for unidirectional laminates, the Hashin criteria have also been applied successfully to progressive failure analyses of laminates by taking into account the constraining interactions between the plies with *in-situ* unidirectional strengths¹⁰. The 2D version of the failure criteria proposed by Hashin in 1973 and 1980 are summarized in Table 1.

Over the past decade, numerous studies have indicated that the stress interactions proposed by Hashin do not always fit the experimental results, especially in the case of matrix or fiber compression. It is well known, for instance, that moderate amounts of transverse compression ($\sigma_{22} < 0$) increases the apparent shear strength of a ply, which is not well predicted by Hashin. In addition, Hashin's fiber compression criterion does not account for the effects of in-plane shear, which reduce significantly the effective compressive strength of a ply. Several authors have proposed modifications to Hashin's criteria to improve their predictive capabilities, two of which are examined below.

Improved Criteria for Matrix Compression

Sun et al.¹¹ proposed an empirical modification to Hashin's 1973 criterion for matrix compression failure to take into account the beneficial role that compressive σ_{22} has on matrix shear strength. The criterion is:

$$\left(\frac{\sigma_{22}}{Y^C}\right)^2 + \left(\frac{\tau_{12}}{S^L - \eta\sigma_{22}}\right)^2 = 1 \quad (1)$$

where η is an experimentally determined constant and may be regarded as an internal material friction parameter. The denominator $S^L - \eta\sigma_{22}$ can be considered an effective in-plane shear strength that increases with transverse compression σ_{22} (see sign convention in Fig. 1). As in Hashin's theories, no attempt was made to calculate the angle of the fracture plane.

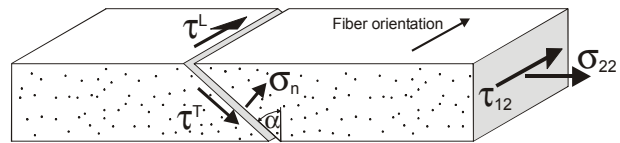


Figure 1. Fracture of a unidirectional lamina subjected to transverse compression and shear.

Table 1. Hashin Criteria^{8,9} for plane stress

Matrix Failure	Matrix tension, $\sigma_{22} \geq 0$ $FI_M = \left(\frac{\sigma_{22}}{Y^T}\right)^2 + \left(\frac{\tau_{12}}{S^L}\right)^2$	Matrix compression, $\sigma_{22} < 0$ 1973: $FI_M = \left(\frac{\sigma_{22}}{Y^C}\right)^2 + \left(\frac{\tau_{12}}{S^L}\right)^2$ 1980: $FI_M = \left(\frac{\sigma_{22}}{2S^T}\right)^2 + \left[\left(\frac{Y^C}{2S^T}\right)^2 - 1\right] \frac{\sigma_{22}}{Y^C} + \left(\frac{\tau_{12}}{S^L}\right)^2$
Fiber Failure	Fiber tension, $\sigma_{11} \geq 0$ $FI_F = \left(\frac{\sigma_{11}}{X^T}\right)^2 + \left(\frac{\tau_{12}}{S^L}\right)^2$	Fiber compression, $\sigma_{11} < 0$ $FI_F = \frac{\sigma_{11}}{X^C}$

where,

FI = Failure Index, with the subscripts M and F indicating matrix and fiber failure, respectively

σ_{ij} = components of normal and shear stresses, with $i, j = 1, 2$

X^T, X^C = strength in fiber direction under tension and compression, respectively (Longitudinal strength)

Y^T, Y^C = strength normal to the fiber direction under tension and compression, respectively (Transverse strength)

S^L and S^T are the in-plane and transverse shear strengths, respectively.

Puck's action plane proposal⁵ represents the beneficial influence of transverse compression on matrix shear strength by increasing the shear strength by a term proportional to the normal stress σ_n acting at the fracture plane shown in Fig. 1. In this formulation, the matrix failure criterion under transverse compression is:

$$\left(\frac{\tau^T}{S^T - \eta^T \sigma_n}\right)^2 + \left(\frac{\tau^L}{S^L - \eta^L \sigma_n}\right)^2 = 1 \quad (2)$$

In Eq. 2, the direct contribution of σ_{22} has been eliminated by assuming that the initiation of fracture at the failure plane is independent of the transverse compressive strength. Internal material friction is characterized by the coefficients η^L and η^T , which are determined experimentally.

One key to Puck's proposal is the calculation of the angle of the fracture plane, α , shown in Fig. 1. Puck determined that matrix failures dominated by in-plane shear occur in a plane that is normal to the ply and parallel to the fibers ($\alpha=0$). For increasing amounts of transverse compression, the angle of the action plane α changes to about 40° , and increases with compression to $53^\circ \pm 2^\circ$ for pure transverse compression. In the WWFE, Puck's predicted failure envelopes correlated very well with the test results⁶. However, the Puck's phenomenological approach uses several material parameters that are not physical and may be difficult to

quantify without considerable experience with a particular material system.

A detailed discussion on Hashin, Puck, Sun and many other criteria has been presented by Paris¹², who also discusses the *ad hoc* nature of the formulation of most strength-based criteria.

LaRC02 Plane Stress Criteria for Matrix Failure

In this section, a new set of criteria is proposed for matrix fracture based on the concepts proposed by Hashin, combined with the fracture plane concept proposed by Puck. In the case of matrix tension, the fracture planes are normal to the plane of the plies and parallel to the fiber direction. The quadratic interaction between in-plane shear and transverse normal tension in Hashin's criterion correlates well with test results. For matrix compression, the plane of fracture may not be normal to the ply, and Hashin was not able to calculate the angle of the plane of fracture. In the present proposal, Mohr-Coulomb effective stresses¹³ are used to calculate the angle of fracture.

Criterion for Matrix Failure in Compression ($\sigma_{22} < 0$)

The Mohr-Coulomb (M-C) criterion¹³ is commonly used in applications where the fracture under tension loading is different from fracture under compression loading, such as in soil mechanics or in the fracture of cast iron. The application of the M-C criterion to

multiaxial failure of epoxy resins was studied by Kawabata¹⁴ based on correlation with his own test results. While studying the failure of chopped glass-fiber/epoxy mat laminates under confining pressures, Boehler¹⁵ found the Tsai-Wu criterion to be inadequate, and formulated a shearing criterion based on the M-C criterion that fit his experimental measurements well. Taliercio¹⁶ used the M-C criterion within a nonlinear micromechanical model to predict the macroscopic strength properties of fiber composites.

The M-C criterion is represented geometrically by the diagram illustrated in Fig. 2. The Mohr's circle represents a state of uniaxial compression. The angle of the plane of fracture α_0 is chosen here to be 53° , which is a typical fracture angle for composites [Puck⁵]. The line AB is the tangent to Mohr's circle at A and is called the Coulomb fracture line. The M-C criterion postulates that in a state of biaxial normal stress, fracture occurs for any Mohr's circle that is tangent to the Coulomb fracture line. The effective stress τ_{eff} is related to the stresses τ^T and σ_n acting on the fracture plane by the expression $\tau_{eff} = \tau^T + \eta\sigma_n$. In the literature, $\tan^{-1}(\eta)$ is called the angle of internal friction and it is assumed to be a material constant. When $\eta=0$, the M-C criterion is equivalent to the Tresca condition.¹³

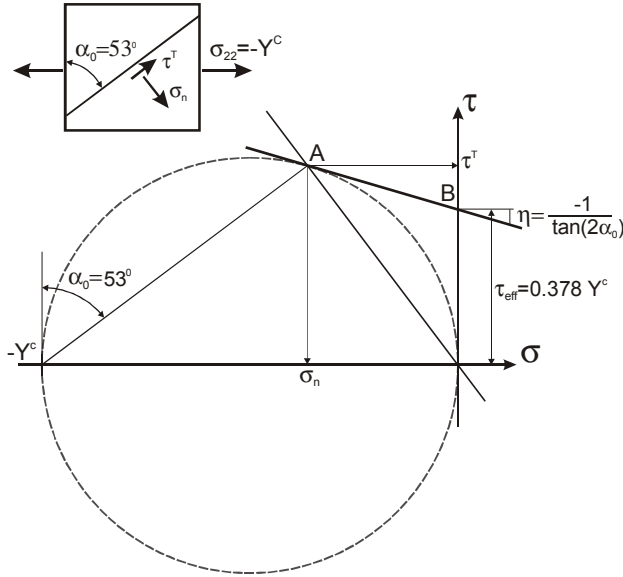


Figure 2. Mohr's circle for uniaxial compression and the effective transverse shear.

DiLandro¹⁷ explains the role of internal friction on the strength of carbon-fiber composites by noting the absence of chemical bonds between fiber and matrix, and that adhesion is attributed to the Van der Waal's interactions. When subjected to an external load, the shear slipping of the two phases is prevented until the shear stress at the fiber-matrix interface reaches a limiting value. DiLandro also notes that η is an empirical factor that encompasses all chemical-physical interactions, including the thermal residual shrinkage of the matrix around the fiber. Larson¹⁸ examined the relative effects of interfacial friction and roughness on the length of interfacial sliding which proceeds from the tip of an impinging fracture oriented perpendicular to the interface. According to Larson, sliding is key to the cracking behavior of fibrous brittle matrix composites in that it affects the stress concentration on the fibers, the matrix crack spacing, and, therefore, the global toughness of a composite material.

In general, the fracture plane can be subjected to transverse as well as in-plane stresses, in which case effective stresses must be defined in both orthogonal directions as shown in Eq. 3.

$$\begin{aligned}\tau_{eff}^T &= \langle |\tau^T| + \eta^T \sigma_n \rangle \\ \tau_{eff}^L &= \langle |\tau^L| + \eta^L \sigma_n \rangle\end{aligned}\quad (3)$$

where the terms η^T and η^L are referred to as coefficients of transverse and longitudinal influence, respectively, and the operand $\langle x \rangle = x$ if $x \geq 0$; otherwise $\langle x \rangle = 0$. Matrix failure under compression loading is assumed to result from a quadratic interaction between the effective shear stresses acting on the faces of a fracture plane. The failure index (FI) is written as

$$FI = \left(\frac{\tau_{eff}^T}{S^T} \right)^2 + \left(\frac{\tau_{eff}^L}{S^L} \right)^2 \leq 1 \quad (4)$$

where S^T and S^L are the transverse and in-plane shear strengths, respectively. The stress components acting on the fracture plane can be expressed in terms of the in-plane stresses and the angle of the fracture plane, α (see Fig. 1).

$$\begin{aligned}
\sigma_n &= \cos^2 \alpha \sigma_{22} \\
\tau^T &= -\sin \alpha \cos \alpha \sigma_{22} \\
\tau^L &= \tau_{12} \cos \alpha
\end{aligned} \quad (5)$$

Using Eqs. 3 and 5, the effective stresses for an angle of the fracture plane α between 0° and 90° are

$$\begin{aligned}
\tau_{eff}^T &= \left\langle -\sigma_{22} \cos \alpha (\sin \alpha - \eta^T \cos \alpha) \right\rangle \\
\tau_{eff}^L &= \left\langle \cos \alpha (|\tau_{12}| + \eta^L \sigma_{22} \cos \alpha) \right\rangle
\end{aligned} \quad (6)$$

Calculation of Coefficients η^T and η^L and Strength S^T

The coefficients of influence η^T and η^L are obtained from the case of uniaxial transverse compression ($\sigma_{22} < 0$, $\tau_{12} = 0$). At failure, the in-plane compressive stress is equal to the matrix compressive strength, $\sigma_{22} = -Y^C$. The effective transverse shear stress at failure is

$$\tau_{eff}^T = S^T = Y^C \cos \alpha (\sin \alpha - \eta^T \cos \alpha) \quad (7)$$

Under uniaxial transverse compression, fracture occurs at a fracture angle α_0 that maximizes the effective transverse shear. Taking the derivative of the transverse shear stress, Eq. 7, with respect to α gives

$$\begin{aligned}
\frac{\partial \tau_{eff}^T}{\partial \alpha} &= 0 = -\sin \alpha_0 (\sin \alpha_0 - \eta^T \cos \alpha_0) \\
&\quad + \cos \alpha_0 (\cos \alpha_0 + \eta^T \sin \alpha_0) \\
\Leftrightarrow \cos^2 \alpha_0 - \sin^2 \alpha_0 + 2\eta^T \sin \alpha_0 \cos \alpha_0 &= 0
\end{aligned} \quad (8)$$

Solving Eq. 8 for η^T gives

$$\eta^T = \frac{-1}{\tan 2\alpha_0} \quad (9)$$

Puck⁵ determined that when they are loaded in transverse compression, most unidirectional graphite/epoxy composites fail by transverse shear along a fracture plane oriented at $\alpha_0 = 53^\circ \pm 2^\circ$. Therefore, the coefficient of transverse influence is in the range $0.21 \leq \eta^T \leq 0.36$. Note that if the fracture plane were oriented at $\alpha_0 = 45^\circ$, the coefficient of transverse influence would be equal to zero.

The transverse shear strength S^T is a quantity that is difficult to measure experimentally. However, substituting Eq. 8 into Eq. 7 gives an expression relating

the transverse shear strength to the transverse compressive strength:

$$S^T = Y^C \cos \alpha_0 \left(\sin \alpha_0 + \frac{\cos \alpha_0}{\tan 2\alpha_0} \right) \quad (10)$$

For a typical fracture angle of 53° , $S^T = 0.378 Y^C$, as was shown in Fig. 2. Note that in some textbooks, the transverse shear strength is often approximated as $S^T = 0.5 Y^C$, which implies from Eqs. 7 and 9 that the fracture plane is at $\alpha_0 = 45^\circ$ and that $\eta^T = 0$. Also note that with this approximation, Hashin's 1980 2D criterion for matrix failure in compression becomes identical to his 1973 criterion.

The coefficient of longitudinal influence, η^L , can be determined from shear tests with varying degrees of transverse compression. In the absence of biaxial test data, η^L can be estimated from the in-plane and transverse shear strengths, as proposed by Puck:

$$\begin{aligned}
\frac{\eta^L}{S^L} &= \frac{\eta^T}{S^T} \\
\Rightarrow \eta^L &= \frac{-S^L}{Y^C \cos \alpha_0 (\tan 2\alpha_0 \sin \alpha_0 + \cos \alpha_0)} \\
\Rightarrow \eta^L &= -\frac{S^L \cos 2\alpha_0}{Y^C \cos^2 \alpha_0}
\end{aligned} \quad (11)$$

Determination of the Angle of the Fracture Plane

The angle of the fracture plane for a unidirectional laminate loaded in transverse compression is a material property that is easily obtained from experimental data. However, under combined loads, the angle of the fracture plane is unknown. The correct angle of the fracture plane is the one that maximizes the failure index, FI , in Eq. 4. In the present work, the fracture angle is obtained by searching for the maximum of the failure index (Eq. 4) within a loop over the range of possible fracture angles: $0 < \alpha < \alpha_0$. A graphical representation of matrix failure envelopes at various fracture angles is shown in Fig. 3 for a unidirectional E-Glass/LY556 composite subjected to transverse compression and in-plane shear. As seen in the figure, the fracture angle that maximizes the FI for small transverse stresses is $\alpha = 0^\circ$. When the applied transverse stress σ_{22} has a magnitude equal to approximately 2/3 of the transverse compressive strength, Y^C , the angle of the critical frac-

ture plane switches from $\alpha=0^\circ$ to $\alpha=40^\circ$, and then rapidly increases to $\alpha=\alpha_0$, the angle of fracture for uniaxial transverse compression.

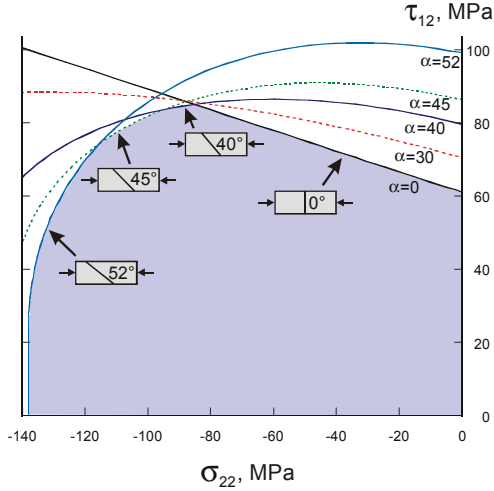


Figure 3. Matrix failure envelopes for a typical unidirectional glass/E. lamina subjected to in-plane compression and shear loading.

Criterion for Matrix Failure in Tension $\sigma_{22} > 0$

Hashin's criterion for matrix tension failure provides adequate predictions of the interaction of in-plane shear and transverse tension for matrix failure. Therefore, the LaRC02 criterion for matrix failure in tension is identical to the criterion proposed by Hashin and is written as

$$FI_M = \left(\frac{\sigma_{22}}{Y^T} \right)^2 + \left(\frac{\tau_{12}}{S^L} \right)^2 \leq 1 \quad (12)$$

LaRC02 Criteria for Fiber Failure

Criterion for Fiber Tension

The LaRC02 criterion for fiber tension failure is a non-interacting maximum allowable strain criterion.

$$\frac{\epsilon_{11}}{\epsilon_1^T} = 1 \quad (13)$$

Criterion for Fiber Compression

Compressive failure of aligned fiber composites occurs from the collapse of the fibers as a result of shear

kinking and damage of the supporting matrix (See for instance the representative works of Fleck¹⁹ and Soutis,²⁰ and Shultheisz²¹ review of micromechanical compressive failure theories). Fiber kinking occurs as shear deformation leading to the formation of a kink band. Argon²² was the first to analyze the kinking phenomenon. His analysis was based on the assumption of a local initial fiber misalignment. The fiber misalignment leads to shearing stresses between fibers that rotate the fibers, increasing the shearing stress and leading to instability.

Since Argon's work, the calculation of the critical kinking stress has been significantly improved with a more complete understanding of the geometry of the kink band as well as the incorporation of friction and material nonlinearity in the analysis models.^{19-21, 23} In the present approach, the compressive strength X^C is assumed to be a known material property that can be used in the LaRC02 matrix damage criterion (Eq. 4) to calculate the fiber misalignment angle that would cause matrix failure under uniaxial compression.

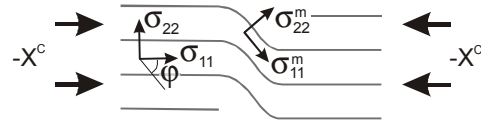


Figure 4. Imperfection in fiber alignment idealized as local region of waviness.

Calculation of Fiber Misalignment Angle

The imperfection in fiber alignment is idealized as a local region of waviness, as shown in Fig. 4. The ply stresses in the misalignment coordinate frame m shown in Fig. 4 are

$$\begin{aligned} \sigma_{11}^m &= \cos^2 \varphi \sigma_{11} + \sin^2 \varphi \sigma_{22} + 2 \sin \varphi \cos \varphi \tau_{12} \\ \sigma_{22}^m &= \sin^2 \varphi \sigma_{11} + \cos^2 \varphi \sigma_{22} - 2 \sin \varphi \cos \varphi \tau_{12} \\ \tau_{12}^m &= -\sin \varphi \cos \varphi \sigma_{11} + \sin \varphi \cos \varphi \sigma_{22} \\ &\quad + (\cos^2 \varphi - \sin^2 \varphi) \tau_{12} \end{aligned} \quad (14)$$

At failure under axial compression, $\sigma_{11} = -X^C$, and $\sigma_{22} = \tau_{12} = 0$. Substituting those values into Eq. 14 gives $\sigma_{22}^m = -\sin^2 \varphi X^C$ and $\tau_{12}^m = \sin \varphi \cos \varphi X^C$,

where the angle φ^C is the misalignment angle for the case of axial compression loading only.

To calculate the failure index for fiber kinking, the stresses σ_{22}^m and τ_{12}^m are substituted into the criterion for matrix compression failure (Eq. 4). The mode of failure in fiber kinking is dominated by the shear stress τ_{12} , rather than by the transverse stress σ_{22} . The angle of the fracture plane is then equal to 0° , and $\tau_{eff}^T = 0$. The matrix failure criterion becomes

$$\tau_{eff}^L = X^C (\sin \varphi^C \cos \varphi^C - \eta^L \sin^2 \varphi^C) = S^L \quad (15)$$

Solving for φ^C leads to the quadratic equation:

$$\tan^2 \varphi^C \left(\frac{S^L}{X^C} + \eta^L \right) - \tan \varphi^C + \left(\frac{S^L}{X^C} \right) = 0 \quad (16)$$

The smaller of the two roots of Eq. 16 is

$$\varphi^C = \tan^{-1} \left(\frac{1 - \sqrt{1 - 4 \left(\frac{S^L}{X^C} + \eta^L \right) \left(\frac{S^L}{X^C} \right)}}{2 \left(\frac{S^L}{X^C} + \eta^L \right)} \right) \quad (17)$$

Note that if η^L were neglected and φ were assumed to be a small constant angle, Eq. 15 would give $\varphi^C \approx \frac{S^L}{X^C}$,

which is the expression derived by Argon²² to estimate the fiber misalignment angle.

The total misalignment angle φ can be decomposed into an initial (constant) misalignment angle φ^0 that represents a manufacturing imperfection, and an additional rotational component φ^R that results from shear loading. The angles φ^0 and φ^R can be calculated using small angle approximations and Eqs. 14

$$\begin{aligned} \varphi^R &= \frac{\tau_{12}^m}{G_{12}} = \frac{-\varphi \sigma_{11} + \varphi \sigma_{22} + (1 - \varphi^2) \tau_{12}}{G_{12}} \\ \varphi^0 &= \varphi^C - \varphi^R \Big|_{X^C} = \varphi^C - \frac{\tau_{12}^m}{G_{12}} \Big|_{X^C} \\ \Rightarrow \varphi^0 &= \varphi^C \left(1 - \frac{X^C}{G_{12}} \right) \end{aligned} \quad (18)$$

Since $\varphi = \varphi^0 + \varphi^R$, it is now possible to solve Eqs. 18 for φ in terms of φ^C .

$$\varphi = \frac{\tau_{12} + (G_{12} - X^C) \varphi^C}{G_{12} + \sigma_{11} - \sigma_{22}} \quad (19)$$

Fiber compression failure by formation of a kink band is predicted using the stresses from Eq. 14 and the failure criterion for matrix tension or matrix compression. For matrix compression ($\sigma_{22}^m < 0$), the criterion is the Mohr-Coulomb criterion given in Eq. 4, with $\alpha=0^\circ$ and $\tau_{eff}^T = 0$. The criterion for fiber kinking becomes:

$$FI_F = \left\langle \frac{|\tau_{12}^m| + \eta^L \sigma_{22}^m}{S^L} \right\rangle \quad (20)$$

For fiber compression with matrix tension, the transformed stresses of Eq. 14 are substituted into the matrix tensile failure criterion given in Eq. 12 to get the following criterion for fiber kinking:

$$FI_F = \left(\frac{\sigma_{22}^m}{Y^T} \right)^2 + \left(\frac{\tau_{12}^m}{S^L} \right)^2 \quad (21)$$

It is interesting to note that for $\sigma_{22} = 0$, the fiber failure criterion in Eq. 20 becomes

$$\begin{aligned} FI_F &= \frac{-\sigma_{11}}{X^C} + \frac{|\tau_{12}|}{k S^L} \\ \text{with } k &= \frac{1}{1 - \varphi^2 - 2\eta^L \varphi} > 1 \end{aligned} \quad (22)$$

The linear interaction between σ_{11} and τ_{12} in Eq. 22 is identical to the form used by Edge for the WWFE⁷. For T300/914C, Edge suggests using an empirical value of $k=1.5$. However, Edge also indicates that other researchers have shown excellent correlation with experimental results with $k=1$. Using the WWFE strength values of $X^C=900$ MPa, $S^L=80$ MPa, $Y^C=200$ MPa; an assumed fracture angle in transverse compression of 53° ; and Eqs. 10 and 17; we get: $\eta^L=0.304$, $\varphi^C=5.3^\circ$. With the approximation $\varphi \approx \varphi^C$, Eq. 22 gives $k=1.07$.

Matrix Damage in Biaxial Compression

In the presence of high transverse compression combined with moderate fiber compression, matrix damage can occur without the formation of kink bands

or damage to the fibers. This matrix damage mode is calculated using the stresses in the misaligned frame in the failure criterion in Eq. 4, which gives:

$$FI_M = \left(\frac{\tau_{eff}^{mT}}{S^T} \right)^2 + \left(\frac{\tau_{eff}^{mL}}{S^L} \right)^2 \quad (23)$$

As for all matrix compressive failures herein, the stresses τ_{eff}^{mT} and τ_{eff}^{mL} are functions of the fracture angle α , which must be determined iteratively.

All the failure modes represented by LaRC02 in Eqs. 3-23 (see also the Appendix) can be represented in a failure envelope in the σ_{11} - σ_{22} plane. An example is shown in Fig. 5 for a 0° E-glass/MY750 epoxy lamina. Puck's analysis results, which showed the best correlation with experimental results in the WWFE³, is also shown for comparison. In the figure, there is good agreement between LaRC02 and Puck in all quadrants except biaxial compression, where LaRC02 predicts an increase of the axial compressive strength with increasing transverse compression. Testing for biaxial loads presents a number of complexities, and experimental results are rare. However, Waas et al.²⁴ present a number of references in which multiaxial compression was studied by superposing a hydrostatic pressure in addition to the compressive loading. For all materials considered, there is a significant increase in compressive strength with increasing pressure. In particular, the results of Wronsky and Parry²⁵ on glass/epoxy show a strength increase of 3.3 MPa per MPa of hydrostatic pressure, which gives an actual strength increase of 4.3 MPa per MPa of applied transverse biaxial stress. More recently, Sigley et al.²⁶ found 32% to 71% increases in compressive strength per 100 MPa superposed pressure. The results of Wronsky and Sigley can be compared qualitatively to the 4.3 MPa/MPa increase in compressive strength for the *plane stress* failure envelope in Fig. 5.

Verification Problems

Example 1. Unidirectional composite E-Glass/LY556

A comparison of results from various failure criteria with the experimental results in the σ_{22} - τ_{12} stress plane obtained from the WWFE²⁷ is shown in Fig. 6. It can be

observed that within the positive range of σ_{22} , all the quadratic failure criteria and LaRC02 give satisfactory results. Since the Maximum Stress criterion does not prescribe interactions between stress components, its failure envelope is rectangular. The most interesting behavior develops when σ_{22} becomes compressive. Hashin's 1973 criterion gives an elliptical envelope with diminishing τ_{12} as compressive σ_{22} increases, while the experimental data shows a definite trend of shear strength increase as σ_{22} goes into compression.

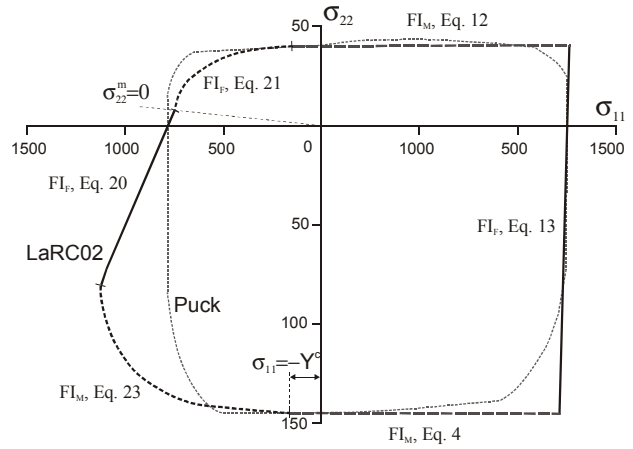
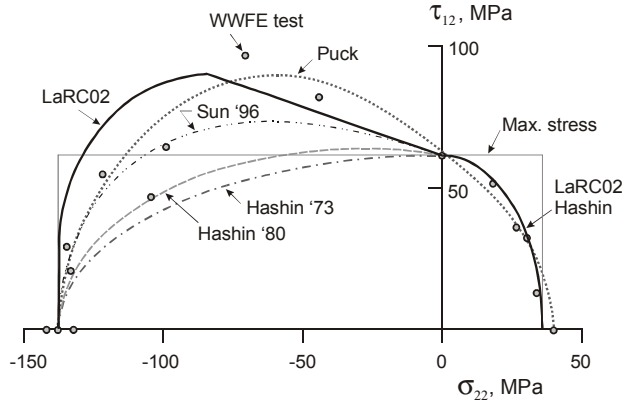


Figure 5. Biaxial σ_{11} - σ_{22} failure envelope of 0° E-glass/MY750 epoxy lamina.

The envelope for Hashin's 1980 criteria was calculated using a transverse strength obtained from Eq. 9, and it provides a modest improvement in accuracy compared to the 1973 criterion. Of the criteria shown in Fig. 6, Sun (Eq. 1), LaRC02 (Eq. 4), and Puck (Eq. 2) capture the shear strength increase at the initial stage of compressive σ_{22} . The failure envelope for Sun's criterion (Eq. 1) was calculated using $\eta^I=0.336$ from Eq. 10. The results indicate a significant improvement over Hashin's criteria. An even better fit would have been achieved using higher value for η^I . Puck's envelope, which was extracted from the 2002 WWFE⁶, is the most accurate, but it relies on fitting parameters based on the same test data. The LaRC02 curve uses the stiffnesses and strengths shown in Table 2, an assumed $\alpha_0=53^\circ$, and no other empirical or fitting parameter.

Table 2. Properties of E-Glass/LY556²⁷ (MPa)

E_{11}	E_{22}	G_{12}	ν_{12}	Y^T	Y^C	S^L
53,480	17,700	5,830	0.278	36	138	61

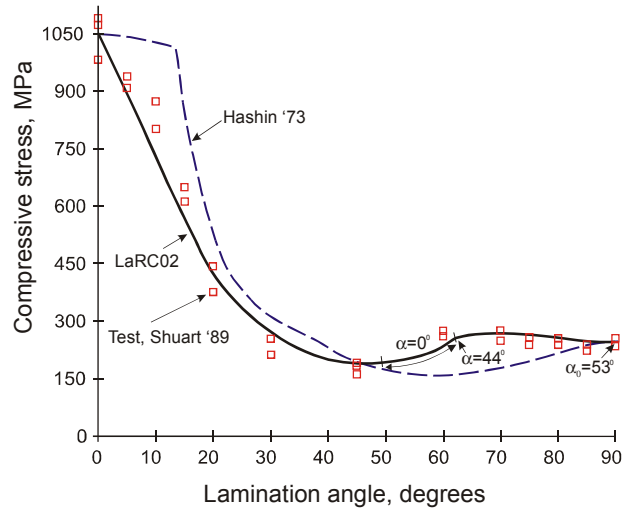
**Figure 6.** Failure envelopes and WWFE test data² for unidirectional composite E-Glass/LY556.

Example 2. Cross-ply laminates

Shuart²⁸ studied the compression failure of $[\pm\theta]_s$ laminates and found that for $\theta < 15^\circ$, the dominant failure mode in these laminates is interlaminar shearing; for $15^\circ < \theta < 50^\circ$, it is in-plane matrix shearing; and for $\theta > 50^\circ$, it is matrix compression. Fiber scissoring due to matrix material nonlinearity caused the switch in failure mode from in-plane matrix shearing to matrix compression failure at larger lamination angles. The material properties shown in Table 3 were used for the analysis. The angle α_0 was assumed to be a typical 53° . For other lamination angles, the fracture angle was obtained by searching numerically for the angle that maximizes the failure criterion in Eq. 4. The results in Fig. 7 indicate that the predicted strengths using LaRC02 criteria correlate well with the experimental results. The compressive strength predicted using Hashin 1973 criteria is also shown in Fig. 7. For $\theta < 20^\circ$, the Hashin criteria result in an overprediction of the failure load because the criterion does not account for the effect of inplane shear on fiber failure. For lamination angles near 70° , the use of the Hashin criteria result in an underprediction of the failure load because the criteria do not account for the increase in shear strength caused by transverse compression.

Table 3. Properties of AS4-3502²⁸ (MPa)

E_{11}	E_{22}	G_{12}	ν_{12}	X^C	Y^C	S^L
127,600	11,300	6,00	0.278	1045	244	95

**Figure 7.** Compressive strength as a function of ply orientation for $[\pm\theta]_s$ AS4/3502 laminates.

Concluding Remarks

The results of the recently concluded World Wide Failure Exercise indicate that the existing knowledge on failure mechanisms needs further development. Many of the existing failure models could not predict the experimental response within a tolerable limit. In fact, differences of up to an order of magnitude between the predicted and experimental values were not uncommon. In this paper, a new set of physics-based failure criteria devoid of empirical variables is proposed. The criteria for matrix and fiber compression failure are based on a Mohr-Coulomb interaction of the stresses associated with the plane of fracture. Failure envelopes for unidirectional laminates in the σ_{11} - σ_{22} and σ_{22} - τ_{12} stress planes were calculated, as well as the compressive strength of cross-ply laminates. The predicted failure envelopes indicate good correlation with experimental results. The proposed criteria represent a significant improvement over the commonly used Hashin criteria, especially in the cases of matrix or fiber failure in compression.

References

- 1) Soden, P.D., Hinton, M.J., and Kaddour, A.S., "A Comparison of the Predictive Capabilities of Current Failure Theories for Composite Laminates," *Composites Science and Technology*, Vol. 58, No. 7, 1998, pp. 1225-1254.
- 2) Soden, P.D., Hinton, M.J., and Kaddour, A.S., "Biaxial Test Results for Strength and Deformation of a Range of E-Glass and Carbon Fibre Reinforced Composite Laminates: Failure Exercise Benchmark Data," *Composites Science and Technology*, Vol. 62, No. 12-13, 2002, pp. 1489-1514.
- 3) Hinton, M.J., Kaddour, A.S., and Soden, P.D., "A Comparison of the Predictive Capabilities of Current Failure Theories for Composite Laminates, Judged against Experimental Evidence," *Composites Science and Technology*, Vol. 62, No. 12-13, 2002, pp. 1725-1797.
- 4) Hinton, M.J., and Soden, P.D., "Predicting Failure in Composite Laminates: The Background to the Exercise," *Composites Science and Technology*, Vol. 58, No. 7, 1998, pp. 1001-1010.
- 5) Puck, A., and Schurmann, H., "Failure Analysis of FRP Laminates by Means of Physically Based Phenomenological Models," *Composites Science and Technology*, Vol. 58, No. 7, 1998, pp. 1045-1067.
- 6) Puck, A., and Schurmann, H., "Failure Analysis of FRP Laminates by Means of Physically Based Phenomenological Models," *Composites Science and Technology*, Vol. 62, No. 12-13, 2002, pp. 1633-1662.
- 7) Edge, E.C., "Stress-Based Grant-Sanders Method for Predicting Failure of Composite Laminates," *Composites Science and Technology*, Vol. 58, No. 7, 1998, pp. 1033-1041.
- 8) Hashin, Z., and Rotem, A., "A Fatigue Criterion for Fiber-Reinforced Materials," *Journal of Composite Materials*, Vol. 7, 1973, pp. 448-464.
- 9) Hashin, Z., "Failure Criteria for Unidirectional Fiber Composites," *Journal of Applied Mechanics*, Vol. 47, 1980, pp. 329-334.
- 10) Shahid, I., and Chang, F.-K., "An Accumulative Damage Model for Tensile and Shear Failures of Laminated Composite Plates," *Journal of Composite Materials*, Vol. 29, 1995, pp. 926-981.
- 11) Sun, C.T., Quinn, B.J., and Oplinger, D.W., "Comparative Evaluation of Failure Analysis Methods for Composite Laminates," DOT/FAA/AR-95/109, 1996.
- 12) Paris, F., "A Study of Failure Criteria of Fibrous Composite Materials," NASA/CR-2001-210661, Hampton, VA, March 2001.
- 13) Salençon, J., *Handbook of Continuum Mechanics: General Concepts, Thermoelasticity*, Springer, Berlin; New York, 2001.
- 14) Kawabata, S., "Strength of Epoxy Resin under Multiaxial Stress Field," *Proceedings of the ICCM-IV*, Tokyo, 1982, pp. 161-168.
- 15) Boehler, J.P., and Raclin, J., "Failure Criteria for Glass-Fiber Reinforced Composites under Confining Pressure," *J. Struct. Mech.*, Vol. 13, No. 3 & 4, 1985, pp. 371-392.
- 16) Taliercio, A., and Sagramoso, P., "Uniaxial Strength of Polymeric-Matrix Fibrous Composites Predicted through a Homogenization Approach," *International Journal of Solids and Structures*, Vol. 32, No. 14, 1995, pp. 2095-2123.
- 17) DiLandro, L., and Pegoraro, M., "Carbon Fibre-Thermoplastic Matrix Adhesion," *Journal of Material Science*, Vol. 22, 1987, pp. 1980-1986.
- 18) Larson, M.C., and Miles, H.F., "On the Effects of Friction, Roughness and Toughness on Interfacial Sliding in Brittle Composites," *Mechanics of Materials*, Vol. 27, No. 2, 1998, pp. 77-89.
- 19) Fleck, N.A., and Liu, D., "Microbuckle Initiation from a Patch of Large Amplitude Fibre Waviness in a Composite under Compression and Bending," *European Journal of Mechanics - A/Solids*, Vol. 20, No. 1, 2001, pp. 23-37.
- 20) Soutis, C., Smith, F.C., and Matthews, F.L., "Predicting the Compressive Engineering Performance of Carbon Fibre-Reinforced Plastics," *Composites Part A: Applied Science and Manufacturing*, Vol. 31, No. 6, 2000, pp. 531-536.
- 21) Schultheisz, C.R., and Waas, A.M., "Compressive Failure of Composites, Part 1: Testing and Micromechanical Theories," *Progress in Aerospace Sciences*, Vol. 32, 1996, pp. 1-42.
- 22) Argon, A.S., *Fracture of Composites*, *Treatise of Materials Science and Technology*, Vol. 1, Academic Press, New York, 1972.
- 23) Budiansky, B., Fleck, N.A., and Amazigo, J.C., "On Kink-Band Propagation in Fiber Composites," *Journal of the Mechanics and Physics of Solids*, Vol. 46, No. 9, 1998, pp. 1637-1653.
- 24) Waas, A.M., and Schultheisz, C.R., "Compressive Failure of Composites, Part II: Experimental Studies," *Progress in Aerospace Sciences*, Vol. 32, No. 1, 1996, pp. 43-78.

- 25) Wronski, A.S., and Parry, T.V., "Compressive Failure and Kinking in Uniaxially Aligned Glass-Resin Composite under Superposed Hydrostatic Pressure," Journal of Material Science, Vol. 17, 1982, pp. 3656-3662.
- 26) Sigley, R.H., Wronski, A.S., and Parry, T.V., "Axial Compressive Failure of Glass-Fibre Polyester Composites under Superposed Hydrostatic Pressure: Influence of Fibre Bundle Size," Composite Science and Technology, Vol. 43, 1992, pp. 171-183.
- 27) Soden, P.D., Hinton, M.J., and Kaddour, A.S., "Lamina Properties, Lay-up Configurations and Loading Conditions for a Range of Fibre-Reinforced Composite Laminates," Composites Science and Technology, Vol. 58, No. 7, 1998, pp. 1011-1022.
- 28) Shuart, M.J., "Failure of Compression-Loaded Multidirectional Composite Laminates," AIAA Journal, Vol. 27, No. 9, 1989, pp. 1274-1279.

Appendix

Table A1. Summary of LaRC02 criteria for plane stress.

Matrix Cracking	Matrix tension, $\sigma_{22} \geq 0$	Matrix compression, $\sigma_{22} < 0$	
		$\sigma_{11} < Y^C$	$\sigma_{11} \geq Y^C$
	$FI_M = \left(\frac{\sigma_{22}}{Y^T}\right)^2 + \left(\frac{\tau_{12}}{S^L}\right)^2$	$FI_M = \left(\frac{\tau_{eff}^{mT}}{S^T}\right)^2 + \left(\frac{\tau_{eff}^{mL}}{S^L}\right)^2$	$FI_M = \left(\frac{\tau_{eff}^T}{S^T}\right)^2 + \left(\frac{\tau_{eff}^L}{S^L}\right)^2$
Fiber Failure	Fiber tension, $\sigma_{11} \geq 0$	Fiber compression, $\sigma_{11} < 0$	
		$\sigma_{22}^m < 0$	$\sigma_{22}^m \geq 0$
	$FI_F = \frac{\epsilon_{11}}{\epsilon_1^T}$	$FI_F = \left\langle \frac{ \tau_{12}^m + \eta^L \sigma_{22}^m}{S^L} \right\rangle$	$FI_F = \left(\frac{\sigma_{22}^m}{Y^T}\right)^2 + \left(\frac{\tau_{12}^m}{S^L}\right)^2$
<p>The effective stresses are $\begin{cases} \tau_{eff}^T = \langle -\sigma_{22} \cos \alpha (\sin \alpha - \eta^T \cos \alpha) \rangle \\ \tau_{eff}^L = \langle \cos \alpha (\tau_{12} + \eta^L \sigma_{22} \cos \alpha) \rangle \end{cases}$</p> <p>The transverse shear strength is $S^T = Y^C \cos \alpha_0 \left(\sin \alpha_0 + \frac{\cos \alpha_0}{\tan 2\alpha_0} \right)$</p> <p>$\eta^T = \frac{-1}{\tan 2\alpha_0}$ and $\eta^L \approx -\frac{S^L \cos 2\alpha_0}{Y^C \cos^2 \alpha_0}$ or from test data.</p> <p>The stresses in the fiber misalignment frame are</p> <p>$\sigma_{11}^m = \cos^2 \varphi \sigma_{11} + \sin^2 \varphi \sigma_{22} + 2 \sin \varphi \cos \varphi \tau_{12}$</p> <p>$\sigma_{22}^m = \sin^2 \varphi \sigma_{11} + \cos^2 \varphi \sigma_{22} - 2 \sin \varphi \cos \varphi \tau_{12}$</p> <p>$\tau_{12}^m = -\sin \varphi \cos \varphi \sigma_{11} + \sin \varphi \cos \varphi \sigma_{22} + (\cos^2 \varphi - \sin^2 \varphi) \tau_{12}$</p> <p>where $\varphi = \frac{\tau_{12} + (G_{12} - X^C)\varphi^C}{G_{12} + \sigma_{11} - \sigma_{22}}$ and $\varphi^C = \tan^{-1} \left(\frac{1 - \sqrt{1 - 4 \left(\frac{S^L}{X^C} + \eta^L \right) \left(\frac{S^L}{X^C} \right)}}{2 \left(\frac{S^L}{X^C} + \eta^L \right)} \right)$</p>			